

# Suppression or enhancement of the Fulde-Ferrell-Larkin-Ovchinnikov order in a one-dimensional optical lattice with particle correlated tunnelling

B. Wang<sup>1,2</sup> and L.-M. Duan<sup>1</sup>

<sup>1</sup>*FOCUS center and MCTP, Department of Physics, University of Michigan, Ann Arbor, MI 48109*

<sup>2</sup>*Condensed Matter Theory Center, Department of Physics, University of Maryland, College Park, MD 20742*

We study through controlled numerical simulation the ground state properties of spin-polarized strongly interacting fermi gas in an anisotropic optical lattice, which is described by an effective one-dimensional general Hubbard model with particle correlated hopping rate. We show that the Fulde-Ferrell-Larkin-Ovchinnikov (FFLO) type of state, while enhanced by a negative correlated hopping rate, can be completely suppressed by positive particle correlated hopping, yielding to an unusual magnetic phase even for particles with on-site attractive interaction. We also find several different phase separation patterns for these atoms in an inhomogeneous harmonic trap, depending on the correlated hopping rate.

PACS numbers:

The recent experimental observation of normal-superfluidity transition in spin-polarized ultra-cold Fermi gas has triggered tremendous interest in this system [1, 2, 3, 4, 5]. In a spin-polarized gas, the competition between the Cooper pairing and the mismatch of Fermi surfaces of different spin species could lead to some exotic quantum phases [6, 7, 8]. On this regard, an example with particular interest is the Fulde-Ferrell-Larkin-Ovchinnikov (FFLO) state, which spontaneously breaks the translational and rotational symmetry in space [6, 7]. The stability region of the FFLO state in three dimensions is unfortunately very narrow [9, 10], and so far it has not been observed in the cold atomic gas. It is much easier to observe the FFLO-like state in a one-dimensional (1D), or quasi-1D gas due to the Fermi surface nesting [11, 12, 13]. The FFLO type of state has been found in 1D systems with a number of theoretical studies on the Hubbard model and its continuous version, including the bosonization approach [14], the Bethe ansatz solution combined with the mean field method [11, 12], and the numerical simulations based on the density matrix renormalization group (DMRG) [15, 16, 17] or the quantum Monte-Carlo [18].

To test the theoretical predictions and observe the FFLO-like states, one needs to have strongly interacting atomic gas confined in an anisotropic optical lattice, where the hopping is basically along only one spatial direction. The strongly interaction introduced by the Feshbach resonance is important for experimentally achieving the low-temperature phase of the system. However, this strongly interaction causes additional complications to the theoretical model Hamiltonian. Because of the multi-band population and the atomic collision over the neighboring sites, the system cannot be described a conventional single-band Hubbard model any more. Instead, based on the analysis of the local Hilbert space structure and the symmetry argument, it is shown in [19, 20] that the effective Hamiltonian for strongly interacting fermions in an optical lattice is described by a general Hubbard model with particle correlated hopping rates.

In this paper, we investigate the possibility to observe the FFLO-like state in the 1D general Hubbard model (GHM) with population imbalance. Note that in an exactly 1D configuration, the state can have only a quasi-long-range (QLO) order with divergence in the corresponding susceptibility. However, this QLO order can be stabilized to a true-long-range order in a quasi-1D configuration with small transverse tunneling [21]. So we can still use the leading QLO order to character the phase of the system. We show that the particle correlated hopping in the general Hubbard model has significant influence on the FFLO phase. While a negative particle correlated hopping rate enhances the stability of the FFLO state, a sufficiently large positive particle correlated hopping rate can completely suppress the FFLO phase and stabilize an unusual spin-density wave (SDW) state (with quasi-long range antiferromagnetic order) even for the atoms with on-site attractive interaction. The solution here is based on controlled numerical simulation with the tensor network algorithm in the thermodynamical limit [22] (a variation of the DMRG method [23]). We also give a analysis of the phase separation pattern for this system in a weak global harmonic trap. While the mean field approach finds a large region of the FFLO state surrounded by a fully paired superfluid state in the wing [11], the exact numerical simulation shows that the parameter window for such a region is very narrow. For the case of the general Hubbard model, more intriguing phase separation patterns could occur. For instance, with positive particle correlation hopping rate, one can have a SDW state at the core and a fully paired superfluid state in the wing, while in between the state of the system shows some remanence of the FFLO-type order.

For strongly interacting fermions near a wide Feshbach resonance, the effective Hamiltonian is given by the following general Hubbard model [19, 20]

$$H = \sum_i [Un_{i\uparrow}n_{i\downarrow} - \mu_{\uparrow}n_{i\uparrow} - \mu_{\downarrow}n_{i\downarrow}] \quad (1)$$

$$- \sum_{\langle i,j \rangle, \sigma} [t + \delta g (n_{i\bar{\sigma}} + n_{j\bar{\sigma}}) + \delta t n_{i\bar{\sigma}} n_{j\bar{\sigma}}] a_{i\sigma}^\dagger a_{j\sigma} + H.c.$$

where  $n_{i\sigma} \equiv a_{i\sigma}^\dagger a_{i\sigma}$  and  $n_i \equiv n_{i\uparrow} + n_{i\downarrow}$  are particle number operators,  $\mu_\sigma$  stands for the chemical potential for the spin- $\sigma$  species,  $\langle i, j \rangle$  denotes the neighboring sites, and  $a_{i\sigma}^\dagger$  is the creation operator to generate a fermion on the site  $i$  with the spin index  $\sigma$ . The symbol  $\bar{\sigma}$  stands for  $(\downarrow, \uparrow)$  given  $\sigma = (\uparrow, \downarrow)$ . The  $\delta g$  and  $\delta t$  terms in the Hamiltonian describe the particle correlated hopping, which come from the contributions of the multi-band processes and the direct neighboring coupling of the atoms. As one moves far away from the Feshbach resonance, the correlated hopping terms vanish and the Hamiltonian in Eq. (1) reduces to the conventional Hubbard model. However, near the resonance,  $\delta g$  and  $\delta t$  can be significant compared with the atomic tunneling rate  $t$ . It is interesting to note that a similar form of the Hamiltonian has also been proposed for the high-Tc cuprate materials [24], so the interest in this model is not limited to the system of the strongly interacting atomic gas. In Eq. (1), we keep  $\mu_\uparrow$  and  $\mu_\downarrow$  different, which accounts for the population imbalance in the two spin components.

In this work, we consider an anisotropic optical lattice where the hopping along the  $x, y$  directions are suppressed by the potential barriers. For this effective one-dimensional system, the ground state can be found through the time-evolving block decimation (TEBD) algorithm [22]. For this algorithm, first we transfer the fermions to effective spins through the Jordan-Wigner transformation [25]. Each site has four possible states, denoted by  $|i_s\rangle$  for the  $s$ th site. The coefficient  $c_{i_1 \dots i_n}$  of the ground-state wave function  $|\Psi\rangle = \sum_{i_1=1}^d \dots \sum_{i_n=1}^d c_{i_1 \dots i_n} |i_1 \dots i_n\rangle$  is expressed in the matrix product form:

$$c_{i_1 \dots i_n} = \sum_{\alpha_1, \dots, \alpha_n=1}^{\chi} \Gamma_{\alpha_n \alpha_1}^{[1]i_1} \Gamma_{\alpha_1 \alpha_2}^{[2]i_2} \Gamma_{\alpha_2 \alpha_3}^{[3]i_3} \dots \Gamma_{\alpha_{n-1} \alpha_n}^{[n]i_n}, \quad (2)$$

where  $\Gamma^{[s]i_s}$  denotes the matrix associated with site- $s$  with the matrix dimension  $\chi$ . The lattice is bipartite, and for calculation in the thermodynamical limit, we assume a translational symmetry of the matrix for each sublattice [22, 25]. The matrix is optimized through minimization of the energy with the imaginary time evolution by the Hamiltonian  $H$ . To identify different orders, we calculate the real space spin ( $S_r$ ), density ( $D_r$ ), and pair ( $P_r$ ) correlations and their Fourier transformations  $X_k = 1/\sqrt{M} \sum_{r=0}^{M-1} X_r \cos(kr)$ , where  $M$  is the number of sites involved in the transformation and  $X$  stands for  $S$ ,  $D$ , or  $P$  correlation [25]. The real space correlation functions are defined by

$$\begin{aligned} S_r^m &\equiv \langle \mathbf{s}_i^m \mathbf{s}_{i+r}^m \rangle - \langle \mathbf{s}_i^m \rangle \langle \mathbf{s}_{i+r}^m \rangle, \\ D_r &\equiv \langle n_i n_{i+r} \rangle - \langle n_i \rangle \langle n_{i+r} \rangle, \\ P_r &\equiv \langle a_{i\uparrow} a_{i\downarrow} a_{i+r\downarrow}^\dagger a_{i+r\uparrow}^\dagger \rangle - \langle a_{i\uparrow} a_{i\downarrow} \rangle \langle a_{i+r\downarrow}^\dagger a_{i+r\uparrow}^\dagger \rangle, \end{aligned} \quad (3)$$

where the spin operators associated with site  $i$  is given by  $\mathbf{s}_i^m \equiv a_{i\alpha}^\dagger \sigma_{\alpha\beta}^m a_{i\beta} / 2$  with  $\alpha$  and  $\beta = \downarrow, \uparrow$  and  $\sigma^m$  ( $m =$

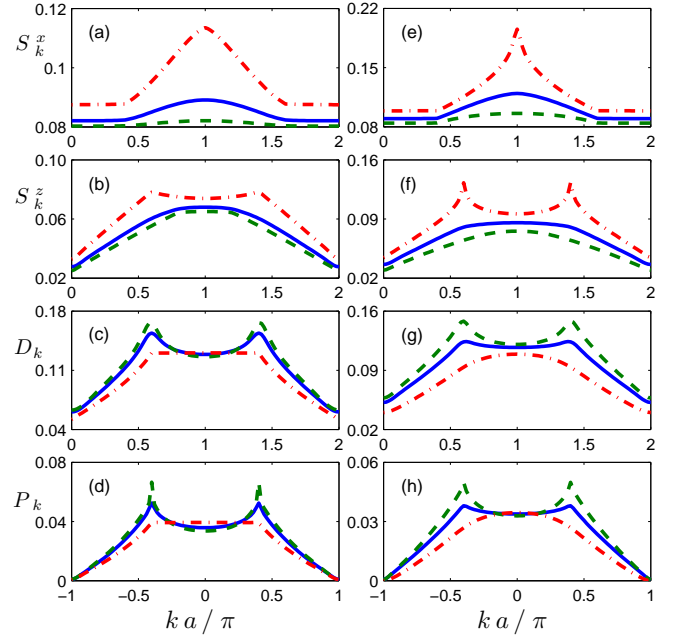


FIG. 1: Fourier transform of the correlation functions for the general Hubbard model at half-filling. For plots (a)-(d),  $U = -8t$ , while  $U = -2t$  for (e)-(h). For all the plots, the spin polarization is chosen to be the same at  $p = 0.4$ . The solid, dashed, and dash-dotted curves correspond to  $\delta g = 0$ ,  $-0.5t$ , and  $t$ , respectively. The parameter  $\delta t$  is taken as  $\delta t = -2\delta g$ .

$x, y, z$ ) standing for the Pauli matrices. In the calculation, we typically take  $\chi = 80$  for the matrix dimension and  $M = 100$  for the Fourier transform (the results have been well converged with the above choice of the parameters).

In Fig. 1, we investigate how the particle correlated hopping rate in the GHM influences the stability of the FFLO state and the phase of the system. In our calculation, we take attractive interaction with  $U = -8t$  and  $-2t$  respectively for the figures on the left and the right panels, and choose a fixed population imbalance with  $p = (N_\uparrow - N_\downarrow) / (N_\uparrow + N_\downarrow) = 0.4$ . First, for the conventional Hubbard model with  $\delta g = \delta t = 0$ , the pair correlation  $P_k$  peaks at nonzero momenta  $k$  with population imbalance, which is a signature of the FFLO like state. The result thus confirms the previous theoretical predictions. Then, we tune the particle correlated hopping rate  $\delta g$ . With a negative  $\delta g$ , as shown in Fig. 1, the peaks of  $P_k$  at non-zero momenta become sharper, which means that the FFLO order gets enhanced (the FFLO is the leading quasi-long-range order in this 1D configuration). However, with a positive  $\delta g$ , the FFLO peaks in the pair correlation  $P_k$  get suppressed, and at  $\delta g = t$ , the peaks in the spin correlation  $S_k$  get more prominent. The peaks in  $S_k$  are particularly sharp with a small on-site attraction  $U = -2t$ , and the spin density wave emerges as the leading quasi-long range order for the system. Although the spin density wave order is expected for the repulsive Hubbard model, its appearance in the case of attractive interaction is unusual since at-

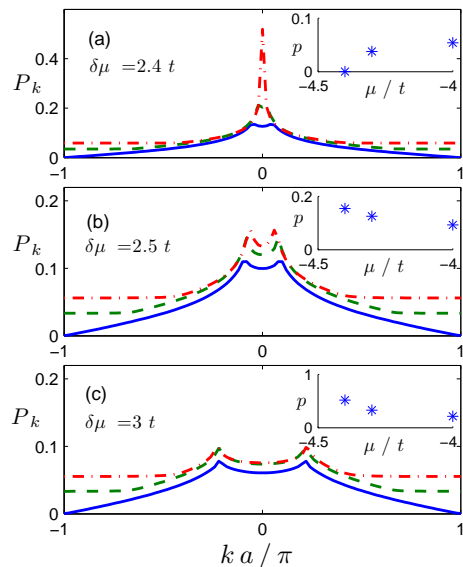


FIG. 2: Pair correlation functions for the conventional Hubbard model at  $U = -8t$ . The difference in chemical potential for spin-up and spin-down species are chosen to be  $\delta\mu \equiv (\mu_\downarrow - \mu_\uparrow)/2 = 2.4t, 2.5t$ , and  $3t$  for plots (a), (b), and (c), respectively. The solid, dashed, and dash-dotted lines in the plots correspond to  $\mu \equiv (\mu_\uparrow + \mu_\downarrow)/2 = -4t$  (half-filling),  $-4.3t$ , and  $-4.4t$ , respectively. The insets show the spin polarization  $p$  corresponding to each curve.

traction normally favors some pairing order. The result of this simulation shows that the particle correlated hopping can cause some qualitative change to the phase of the system.

In the next step, we analyze the possible phase separation patterns for the polarized fermi gas in an inhomogeneous global trap  $V(r)$ . When the trap  $V(r)$  is slowly varying from site to site, we can take the local density approximation where  $V(r)$  basically decreases the local chemical potential from  $\mu$  ( $\mu = (\mu_\uparrow + \mu_\downarrow)/2$ ) to  $\mu - V(r)$  as one moves from the trap center to the edge. So to investigate the qualitative phase separation pattern, we can fix the population imbalance  $p$  (and thus also  $\delta\mu = (\mu_\uparrow - \mu_\downarrow)/2$ ) at the center, and calculate what kind of phases can emerge as one moves to the trap edge. For the conventional Hubbard model, the mean-field theory has predicted a large parameter region where one has a FFLO-like phase at the center, surrounded by a non-polarizing BCS phase at the edge [11]. This separation pattern is somewhat unusual as in the 3-dimensional case, one can only has a BCS phase at the trap center surrounded by other phases (such as FFLO or polarized normal state) at the edge [9, 10]. The recent DMRG calculation however does not find any evidence of this type of phase separation pattern predicted by the mean-field theory [15]. To resolve this problem, we have performed more extensive calculation over a large parameter window. We indeed find that this type of phase separation is possible, however, it exists only for a very narrow pa-

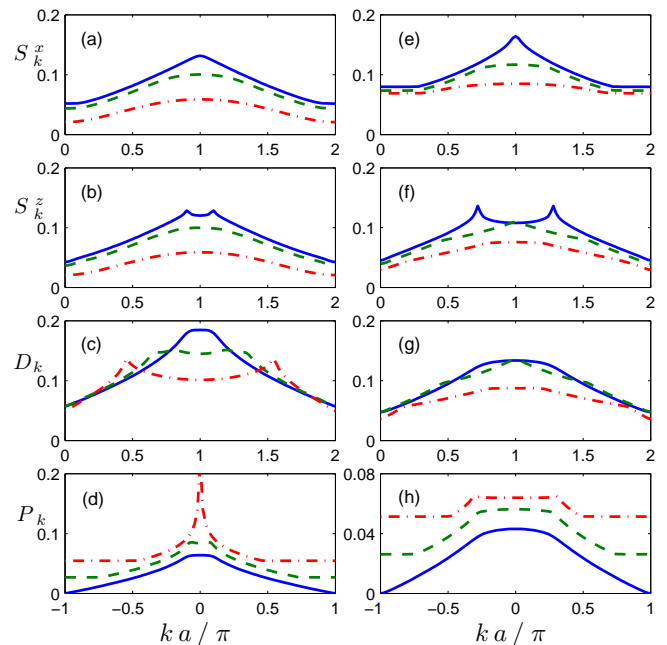


FIG. 3: The correlation functions for the general Hubbard model at  $U/t = -2$ ,  $\delta g/t = 1$  and  $\delta t/t = -2$ . Difference in chemical potentials for spin-up and spin-down species are chosen to be  $\delta\mu \equiv (\mu_\downarrow - \mu_\uparrow)/2 = 1.2t$  and  $2.4t$  for the left and right column, respectively. The solid, dashed, and dash-dotted lines correspond to  $\mu \equiv (\mu_\uparrow + \mu_\downarrow)/2 = -t$  (half-filling),  $-2.5t$ , and  $-3.3t$ , respectively.

parameter window with the region much smaller than the one predicted by the mean-field theory.

In Fig. 2, we show different kinds of phase separation patterns for the conventional Hubbard model with  $U = -8t$ . We take the density about half filling at the trap center and vary the population imbalance there. With a tiny population imbalance at the center (for instance with  $p = 0.054$  in Fig. 2a, with the corresponding  $\delta\mu = 2.4t$ ), when one moves to the edge, the population imbalance  $p$  decreases with decrease of  $\mu$  (see the insert of Fig. 2a), and a non-polarizing BCS state emerges at the edge. However, when one slightly increase the population imbalance at the center (for instance with  $p = 0.093$  in Fig. 2b, with the corresponding  $\delta\mu = 2.5t$ ), the population imbalance increases with a decreasing  $\mu$  as one moves to the edge, and the state finally goes to a polarized normal phase (with no peaks in the correlation function, not shown in Fig. 2). This is different from the mean-field prediction [11], where one could get a non-polarizing BCS state at the edge as long as the central polarization  $p$  is below 0.2. In Fig. 2c, we show the result when the central polarization  $p \approx 0.2$ . Clearly, the polarization is increasing as one moves to the edge (similar to Fig. 2b), and there is no possibility of a BCS state there.

In Fig. 3, we investigate the phase separation pattern for the GHM with particle correlated hopping. The phase separation pattern is of particular interest for the

case of a positive particle correlated hopping rate  $\delta g$ . In this case, at the trap center we have a spin density wave state, while at the edge the state depends on the overall population imbalance of the system. In the case of a large population imbalance (the right panel of Fig. 3), we get a polarized normal state at the edge. However, in the case of a small population imbalance, the spin-density wave state can be accompanied by a non-polarizing BCS state at the edge, as evidenced by the sharp peak in the pair correlation  $P_k$  in Fig. 3d. With a negative particle correlated hopping rate  $\delta g$ , the phase separation pattern is qualitatively similar to the case of the conventional Hubbard model, and thus not shown in Fig. 3.

In summary, through well controlled numerical simu-

lation we have investigated the properties of the attractive general Hubbard model under population imbalance, which describes the strongly interacting fermi gas in a one-dimensional optical lattice. The FFLO type of order gets either enhanced or suppressed depending on the sign of the particle correlated hopping rate  $\delta g$ . When the FFLO state is fully suppressed with a positive  $\delta g$ , we get an unusual spin density wave state. We also investigate the phase separation pattern of the system under a weak inhomogeneous trap, and find several different phase separation patterns depending on the polarization of the system and the particle correlated hopping rates.

This work was supported by the MURI, the DARPA, and the DTO under ARO contracts.

- 
- [1] M. W. Zwierlein, A. Schirotzek, C. H. Schunck, and W. Ketterle, *Science* **311**, 492 (2006).
  - [2] G. B. Partridge et al., "Pairing and phase separation in a polarized Fermi gas", *Science* **311**, 503 (2006).
  - [3] M. W. Zwierlein, C. H. Schunck, A. Schirotzek, and W. Ketterle, *Nature* **442**, 54 (2006).
  - [4] Y. Shin et al., *Phys. Rev. Lett.* **97**, 030401 (2006).
  - [5] G. B. Partridge et al., *Phys. Rev. Lett.* **97**, 190407 (2006).
  - [6] P. Fulde, and R. A. Ferrell, *Phys. Rev.* **135**, A550 (1964).
  - [7] A. I. Larkin, and Yu. N. Ovchinnikov, *Sov. Phys. JETP* **20**, 762 (1965).
  - [8] G. Sarma, *J. Phys. Chem. Solids*, **24**, 1029 (1963).
  - [9] D. E. Sheehy and L. Radzihovsky, *Phys. Rev. Lett.* **96**, 060401 (2006).
  - [10] W. Zhang, L.-M. Duan, *Phys. Rev. A* **76**, 042710 (2007).
  - [11] H. Hu, X.-J. Liu, and P. D. Drummond, *Phys. Rev. Lett.* **98**, 070403 (2007).
  - [12] G. Orso, *Phys. Rev. Lett.* **98**, 070402 (2007).
  - [13] M. M. Parish, S. K. Baur, E. J. Mueller, D. A. Huse, *Phys. Rev. Lett.* **99**, 250403 (2007).
  - [14] K. Yang, *Phys. Rev. B* **63**, 140511(R) (2001).
  - [15] A. E. Feiguin and F. Heidrich-Meisner, *Phys. Rev. B* **76**, 220508(R) (2007).
  - [16] M. Tezuka and M. Ueda, *Phys. Rev. Lett.* **100**, 110403 (2008).
  - [17] M. Rizzi et al., *Phys. Rev. B* **77**, 245105 (2008).
  - [18] G. G. Batrouni, M. H. Huntley, V. G. Rousseau, and R. T. Scalettar, *Phys. Rev. Lett.* **100**, 116405 (2008).
  - [19] L.-M. Duan, *Phys. Rev. Lett.* **95**, 243202 (2005).
  - [20] L.-M. Duan, *Europhys. Lett.* **81**, 20001 (2008).
  - [21] E. W. Carlson, V. J. Emery, S. A. Kivelson, and D. Orgad, "Concepts in high temperature superconductivity", in *The physics of superconductors* (Springer, Berlin, 2003).
  - [22] G. Vidal, *Phys. Rev. Lett.* **98**, 070201 (2007).
  - [23] For a review, see U. Schollwoeck, *Rev. Mod. Phys.* **77**, 259 (2005).
  - [24] M. E. Simon and A. A. Aligia, *Phys. Rev. B* **48**, 7471 (1993).
  - [25] B. Wang and L.-M. Duan, *N. J. Phys.* **10**, 073007 (2008).